A new EXAFS investigation of local structural changes in amorphous and crystalline GeO_2 at high pressure

2009 J. Phys.: Condens. Matter 21 145403

(http://iopscience.iop.org/0953-8984/21/14/145403)

J. Phys.: Condens. Matter **21** (2009) 145403 (8pp) doi:10.1088/0953-8984/21/14/145403

A new EXAFS investigation of local structural changes in amorphous and crystalline GeO_2 at high pressure

M Vaccari, G Aquilanti, S Pascarelli and O Mathon

European Synchrotron Radiation Facility, 6 rue Jules Horowitz, BP 220, 38043 Grenoble Cedex, France

E-mail: vaccari@esrf.fr

Received 8 November 2008, in final form 2 February 2009
Published 9 March 2009
Online at stacks.iop.org/JPhysCM/21/145403

Abstract

Structural transformations at high pressure in amorphous and quartz-like crystalline GeO_2 have been investigated by using a Paris–Edinburgh press coupled to EXAFS spectroscopy. From both the germanium absorption edge position and the Ge–O distance evolution, new detailed information has been obtained about the pressure behavior of the short range order. Crystalline GeO_2 undergoes a transformation from four- to six-fold coordination at about 8.5 GPa, but at least the whole 6–12 GPa pressure range should be considered as the transition region. On the other hand, amorphous GeO_2 is characterized by a much more gradual structural change and the full octahedral state is not reached at 13 GPa as commonly believed. Furthermore, no support to the recently claimed fully pentahedral intermediate state can be given. EXAFS signals of glassy GeO_2 beyond the first Ge–O shell qualitatively confirm the continuous breakdown of the intermediate range order up to 10 GPa.

1. Introduction

The nature of amorphous–amorphous transformations (AATs) under pressure and the concept of poly-amorphism in the classic network-forming glasses such as a-GeO_2 are of fundamental interest in glass theory and represent a strongly debated issue in modern condensed matter physics [1–4]. The occurrence of poly-amorphic transitions at high pressure has been recognized to occur also in a variety of tetrahedral amorphous systems such as Si [5, 6], Ge [7], C [8], SiO_2 [9] and even in glassy carbonia [10, 11] and water [12]. In amorphous solids, transformations with specific features, distinguished from sharp transitions in crystals and melts, are possible. AATs have been claimed to be either 'first order' (i.e. with zero transition width and a discontinuous volume change) or gradual and continuous. Fundamental questions regarding the compactation process itself and the details of coordination changes remain unknown for most AATs and, consequently, are still a matter of discussion [3].

Amorphous GeO_2 is one of the most studied examples of materials for which an AAT occurs at high pressure. Short and medium range structural and vibrational properties of a-GeO_2, even at mere ambient conditions, have been extensively investigated from both experimental [13–19] and theoretical [20–25] points of view. The structural evolution under pressure of crystalline, amorphous and liquid GeO_2 has received increasing attention and it is reviewed in [26]. However, conflicting results were obtained in previous works and, despite two decades of investigations, the details of short range order (SRO) changes are still not well established. A deeper understanding of the behavior of the 'simple' tetrahedral GeO_2 glass is also important as a basis for further investigations on more complex oxide glasses [27–29].

About twenty years ago a Brillouin scattering experiment [30] already guessed the existence of an AAT in a-GeO_2. The well known x-ray absorption spectroscopy (XAS) work of Itié *et al* [31, 32] gave evidence—from the evolution of Ge–O distances and near-edge XANES features—of a rapid change in Ge coordination from four-fold to six-fold between 7 and 9 GPa. A Raman spectroscopic study [33] was consistent with this picture of a structural transformation between 6 and 13 GPa, with no further major changes above this pressure. The XAS result was later more formally interpreted according the so-called two-domain description: the average Ge–O bond length was modeled as a linear combination of pure four- and six- coordinated species ($^{[4]}$Ge and $^{[6]}$Ge, respectively),

using the fitting parameters from equation of state measurements [34]. Changes in Raman [35], Brillouin [36] and infrared measurements [37] were also interpreted as the progress of the AAT from a low-density to a high-density glass. Quite recently a more complex pressure dependence of Ge–O coordination number was argued from x-ray and neutron diffraction measurements [38]: a new metastable, intermediate form of the glass with a constant average coordination of about 5 was observed between about 6 and 10 GPa. Support for this picture was given by density, x-ray scattering and optical Raman measurements [39], which found a density plateau at 6–9 GPa as well as the collapse of all tetrahedral and pentahedral structural units at 13 GPa in favor of a complete octahedral form [39, 40]. These findings were not supported by molecular dynamics (MD) simulations [41–43], which actually showed a substantial number of $^{[5]}$Ge atoms coordinated with five oxygens but did not support the existence of an entirely pentahedrally coordinated state; furthermore, the average Ge–O coordination reached only about 5.2 at 13 GPa, thus not validating the hypothesis of a full transformation to octahedral coordination in this pressure range.

Therefore, the detailed pressure evolution of the local environment of Ge in a-GeO_2 is far from being completely clarified. In order to shed new light on this scenario made up of completely contradictory evidence, new experimental data on the local order of a-GeO_2 are required. Due to its peculiar short range sensitivity and chemical selectivity, Extended x-ray absorption fine structure (EXAFS) is probably the most suitable technique for an investigation of the pressure dependence of Ge–O distance and average coordination. Indeed, by using the large volume Paris–Edinburgh press as a pressure device and the high quality energy scanning XAS beamline BM29 at ESRF, new *in situ* experimental data characterized by a remarkable long energy range and unprecedented accuracy at high pressure have been obtained. The analysis of these data allowed us to eliminate any ambiguity on the structural short range behavior of amorphous GeO_2 under pressure. While the main drawback of such an approach is represented by the maximum pressure reachable (about 13 GPa in this study), the severe energy limitations of diamond anvil cell based EXAFS works at the Ge K-edge (strong glitches coming from diamond Bragg diffraction peaks which contaminate the absorption spectra) are completely avoided.

Structural modifications of a-GeO_2 at an intermediate length scale, and their possible relation with local coordination changes, are also current subjects of investigation [39]. Intermediate range order (IRO) describes the manner in which structural units are assembled into the three-dimensional network of the glass, and it is typically exhibited by systems having AX_2 stoichiometry. In amorphous GeO_2 it is usually recognized through the appearance of a first sharp diffraction peak (FSDP) at $Q \approx 1.5$ Å^{-1} [19] in the structure factor $S(Q)$. The connections between the Boson peak energy in the Raman spectrum to both the features of the FDSP and the intermediate correlation lengths in glasses have been the subject of extended debate also for a-GeO_2 [44–47]. While the aim of this EXAFS study was mainly focused on the SRO properties, some qualitative information is also revealed on the intermediate range order of amorphous GeO_2.

For comparison purposes on the SRO behavior, crystalline GeO_2 has also been studied in the same pressure range as a-GeO_2. Quartz-like q-GeO_2 [48, 49] transforms with pressure to a poorly crystalline monoclinic form (space group $P2_1/c$), consisting of edge-sharing chains of GeO_6 octahedra [50, 51]. An increase of Ge–O distance after 7 GPa was observed from XAS [31, 52] and accordingly interpreted in terms of a tetrahedral to octahedral change in germanium coordination.

The paper is organized as follows. Experimental and data analysis details about the high pressure EXAFS measurements are presented in sections 2 and 3, respectively. Section 4 is devoted to the outline and discussion of the results on crystalline and amorphous GeO_2, which have been critically compared with the findings of previous experimental and theoretical investigations reported in the literature. Finally in section 5 the main conclusions from this work are summarized.

2. Experiment

High purity GeO_2 powders (99.999%, purchased from Aldrich Chemical Co.) have been finely ground using an agate mortar and homogeneously mixed with a suitable quantity of h-BN, which is chemically inert to the materials under study and good pressure transmitting medium, as well as with a small percentage of NaCl. The crystalline and amorphous nature of q- and a-GeO_2 samples was checked by x-ray diffraction. Cylindrical pellets of the sample–matrix mixture were inserted into a 5 mm boron-epoxy gasket. At ambient conditions, the sample thickness was about 20 μm, which provided an edge jump of about 0.8 (increasing up to about 1.2 at high pressure, due to the gasket squeezing).

The EXAFS experiment was performed in transmission mode at the Ge K-edge using the BM29 x-ray absorption spectroscopy beamline [53] of the ESRF (European Synchrotron Radiation Facility). The electron energy and maximum current were 6 GeV and 200 mA, respectively. The high-stability fixed-exit monochromator was equipped with a pair of Si 311 crystals and the primary slit vertical aperture was set to 0.7 mm, thus achieving an energy resolution of about 0.9 eV (the intrinsic core hole energy width at the Ge K-edge is about 2 eV). The harmonic rejection, with rejection level better than 10^{-5}, was obtained using a double reflection on a pair of Si mirrors with grazing incidence of 2 mrad. The lower mirror was bent in order to vertically focus the beam at the sample position. The beam size incident on the sample was about 70 μm and 500 μm vertically and horizontally, respectively. Energy was calibrated by setting the first inflection point of the absorption edge of amorphous germanium (a-Ge) to 11 103 eV. For energy-scale calibration purposes, a reference of a-Ge at ambient conditions was placed after the second ionization chamber and contemporaneously measured during all the experiment. The pre-edge and edge regions were sampled at constant energy steps ΔE of 5 and 0.2 eV, respectively, whereas the EXAFS region was sampled at constant photo-electron wavenumber steps $\Delta k = 0.03$ Å^{-1}. The incoming and outgoing photon fluxes were measured by two ionization chambers filled with

argon (pressure 100 mbar and 600 mbar, respectively). The acquisition time was 4 s/point. Two or three spectra were collected at each pressure, to allow an evaluation of experimental uncertainty.

A Paris–Edinburgh large volume V5 press, equipped with sintered diamond anvils [54], was used as the pressure device. The bi-conical shape of the boron-epoxy gasket coupled with the quasi-conical profiles of the anvils ensured quasi-hydrostatic conditions [54, 55]. In order to determine the pressure *in situ* on the sample, a monochromatic beam (E = 15 keV) was used to collect diffraction rings on a MAR345 image plate (100 μm pixel resolution), mounted in an offset position at about 30 cm from the sample. The sample-detector distance was calibrated by a LaB_6-filled gasket at the sample position. Two-dimensional image plate data were corrected for spatial distortion and integrated with Fit2D [56] to produce a 2θ-I pattern. The well known NaCl Birch–Murnaghan (parameters quoted in [57]) and Vinet [58] equations of state (EOS), as well as h-BN Birch–Murnaghan EOS [59] up to 10 GPa, allowed us to relate the position of diffraction peaks—and therefore lattice parameters—of pressure markers to the real sample pressure, whose uncertainty is conservatively estimated to be $\pm$0.3 GPa. Due to the strong background coming from the boron-epoxy gasket [60] and the considerable sample–matrix dilution, it was impossible to also detect the diffraction signal coming from the GeO_2 sample.

3. Data analysis

The edges of all the normalized a-Ge foil spectra, measured as reference, were aligned to within 0.01 eV and possible slight energy shifts were correspondingly applied to the GeO_2 spectra. All the good spectra collected for each pressure value (typically two or three, but sometimes even more) were averaged in order to improve statistical noise. These steps were performed by using the program ATHENA [61].

The contribution to the absorption coming from all channels other than the Ge K-edge was subtracted through a linear extrapolation of the pre-edge behavior up to about 300 eV before the edge. The normalized absorption spectra in the near-edge (XANES) region at selected pressures are shown in figure 1. The EXAFS signal was obtained as $\chi(k) = (\mu - \mu_0)/\mu_0$, where μ is the experimental absorption coefficient and μ_0 is a smooth spline representing the embedded-atom absorption background. The latter was chosen as a compromise by trying to keep the un-physical low-R part of the Fourier transform as small as possible, while avoiding oscillations in μ_0 itself. The energy to wavevector conversion $k = (2m/\hbar^2)[E - E_b]$ was performed by setting the edge energy E_b to the maximum of the first derivative (or when necessary the zero-crossing of the second derivative was calculated) for each pressure value. The variation of the edge position as a function of pressure is shown in figure 2. These steps were performed by using the program VIPER [62].

The k-weighted EXAFS functions $k^3\chi(k)$ at selected pressures are shown in figure 3 for both crystalline and amorphous GeO_2. The overall quality is excellent and the k-range available for analysis extends up to about 13 Å^{-1}: for higher photo-electron energies, spectra are distorted and the signal-to-noise ratio is poor at the highest pressures. Therefore, an homogeneous set of spectra characterized by the same $k_{max} = 13$ Å^{-1} was considered.

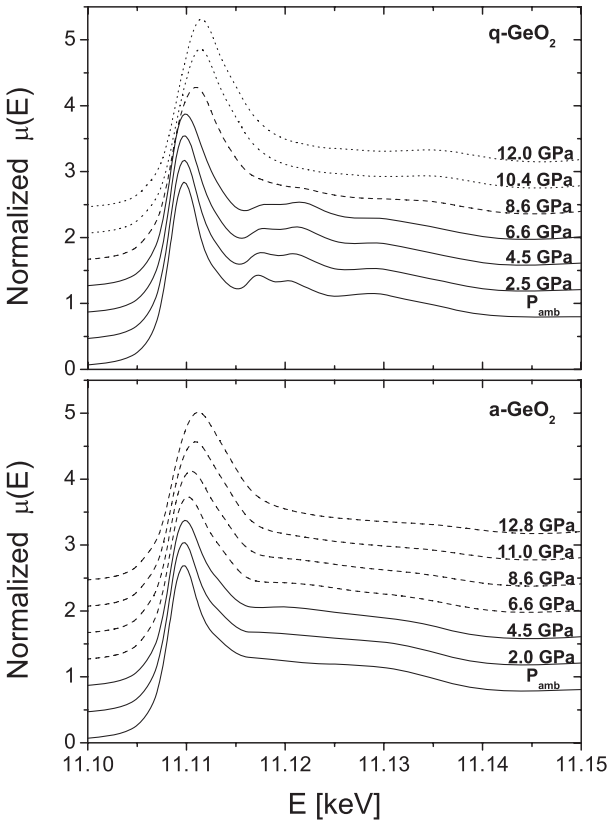

Figure 1. Normalized XANES spectra at the Ge K-edge of crystalline (top panel) and amorphous (bottom panel) GeO_2 at selected pressures. The spectra drawn in continuous line correspond to the low pressure phase, in dashed line to the transition region and in dotted line (only for q-GeO_2) to the high pressure phase.

The EXAFS functions $k^3\chi(k)$ have been Fourier transformed with a Kaiser–Bessel window in the k-range 2.5–13 Å^{-1}. The moduli of Fourier transforms at selected pressures are shown in figure 4. The transforms were performed without phase-shift correction, so the peak positions are backward shifted with respect to the actual interatomic distances. In both compounds, the main peak at about 1.3 Å is due to the nearest neighbor oxygen atoms, which at ambient conditions are tetrahedrally coordinated to the central Ge atom. In crystalline GeO_2 the structure from about 1.8 to 3.4 Å is due—at ambient pressure—to second and third coordination shells (made up of four germanium and six oxygen atoms, respectively) and to multiple scattering contributions. In the case of amorphous GeO_2, a signal beyond the first coordination shell is evident in both figures 3 and 4 (bottom panels) and is explained by the considerable degree of intermediate range order of the glass.

A quantitative analysis has been performed for the Ge–O first shell, whose contribution can be well separated and interpreted within the single scattering framework. This approach is fully justified since at low distances the g_{GeO} partial

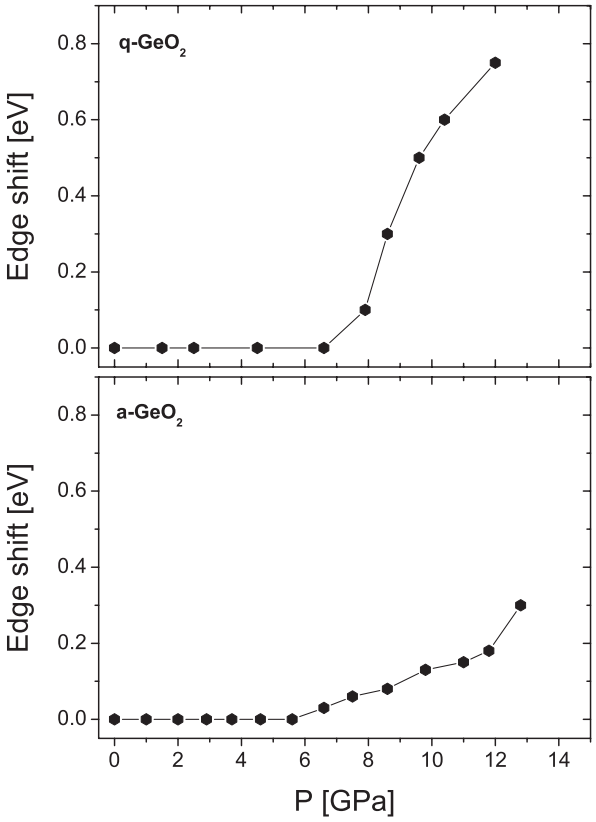

Figure 2. Energy variation of the edge position of crystalline (top panel) and amorphous (bottom panel) GeO_2 as a function of pressure. The edge position was calculated as the zero-crossing of the second derivative of the normalized absorption spectra. The line is only a guide for the eye.

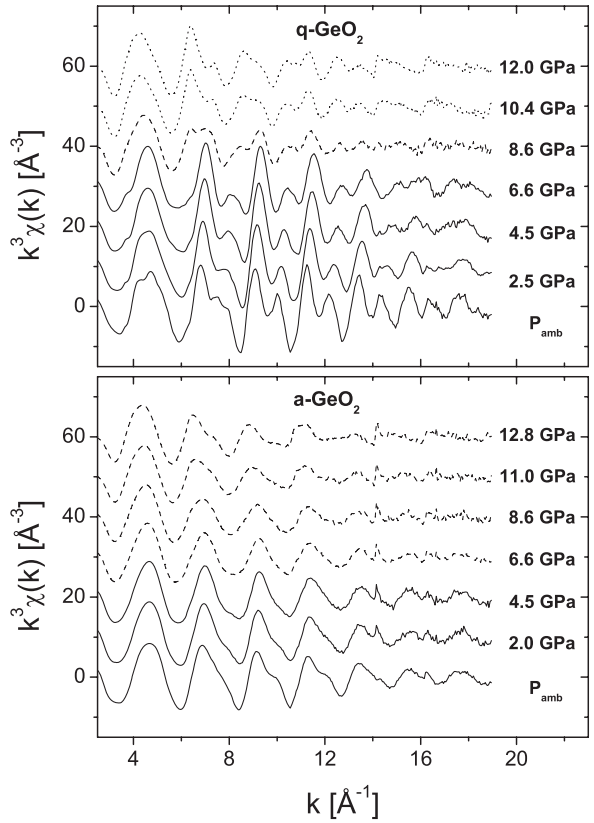

Figure 3. Extracted $k^3\chi(k)$ EXAFS signals of crystalline (top panel) and amorphous (bottom panel) GeO_2 at selected pressures. The spectra are drawn following the same line-styles as in figure 1.

pair distribution function is composed by an isolated peak for both glassy [19, 23] and crystalline GeO_2. Back-scattering amplitudes and phase shifts, as well as the photo-electron mean free path, were calculated by FEFF6 for a tetrahedral Ge–O configuration and a non-linear best-fit to experimental data was performed by using the program ARTEMIS [61, 63]. The fitting interval in R-space was 0.6–1.8 Å and a typical fit is shown in figure 5 in both R-space and back-transformed q-space (inset of figure 5). Data were interpreted in terms of a symmetric distribution of Ge–O distances and the free parameters were its mean value R, variance σ^2 (the term $\exp\{-2k^2\sigma^2\}$ is the so-called EXAFS Debye–Waller factor) and normalization given by the coordination number N. The possible influence of an asymmetry term was checked but it did not significantly affect the pressure evolution of the Ge–O distance. Two further non-structural parameters were treated as follows: the amplitude reduction factor S_0^2 was set (typically to about 1.1) by imposing a coordination number $N = 4$ at ambient pressure, while the energy mismatch e_0 between experimental and theoretical scales was set to the value (about 5.4 eV) found at the lowest pressures. In figure 6 the first shell Ge–O average bond length is shown, for both q- and a-GeO_2, as a function of pressure up to about 13 GPa: it represents the main result of this work and will be discussed below. The absolute value of R_{Ge-O} at ambient pressure (here it was found to be about 1.745 Å) should be taken with caution: it is well known that theoretical phase shifts and experimental energy scales can induce possible systematic errors of the order of 0.01 Å, therefore only the distance variation as a function of an external parameter (pressure in this case) can be considered accurate. Amplitudes of EXAFS signal are much more problematic to treat in high pressure experiments: the extremely high correlations between the two fitting parameters N and σ^2 prevent their reliable determination, since the limited good k-range of data makes it difficult to determine the correct decay of EXAFS oscillations. Furthermore, as described in section 2, the sample is characterized by a cylindrical shape, which introduces unavoidable experimental distortions in EXAFS amplitude with respect, for example, to a standard flat pellet. Finally, the squeezing process makes the sample profile change at every pressure value and this critically affects the homogeneity of the sample itself. Therefore, caution should be used in considering the exact values of coordination number N and the disorder parameter σ^2 (figures 7 and 8, respectively).

4. Results and discussion

4.1. Quartz-like GeO_2

The absorption edge position (figure 2, top panel) was found to be 11 108.4 eV at ambient conditions (in agreement with [64]) and it undergoes a sharp increase in the transition region at

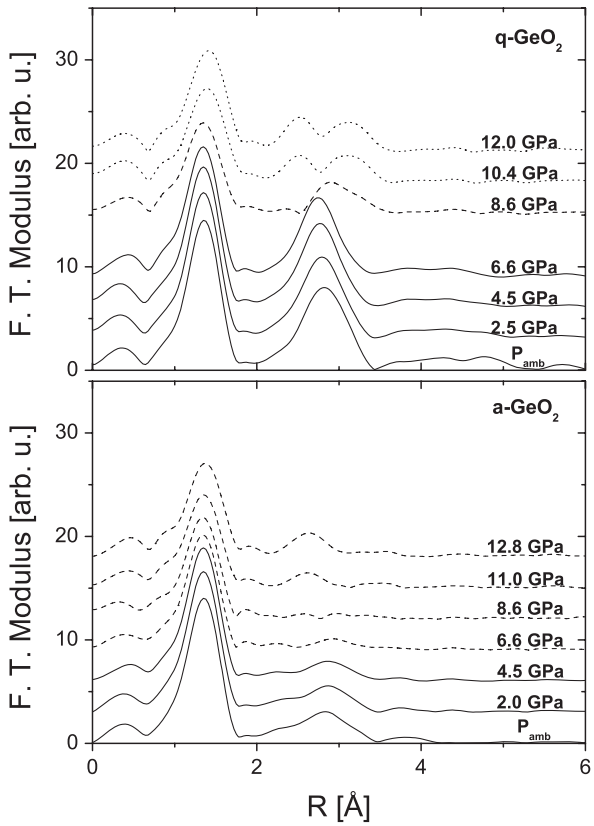

Figure 4. Fourier transform modulus of the EXAFS signals of crystalline (top panel) and amorphous (bottom panel) GeO_2 at selected pressures. The spectra are drawn following the same line-styles as in figure 1.

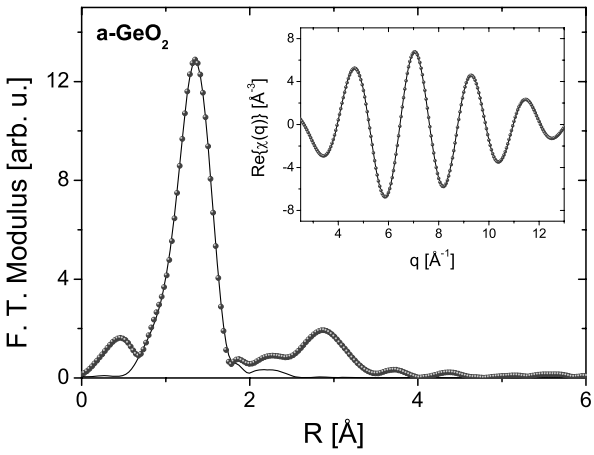

Figure 5. Comparison between experimental data (full circles) and best-fit calculation (continuous line) in the case of a-GeO_2 at 4.5 GPa. The main figure shows the comparison of the moduli of the Fourier transforms (R-space), while in the inset the back-transformed signals (q-space) corresponding to the first coordination shell are reported.

about 6–12 GPa. This behavior is qualitatively compatible with the energy shift of about +1.2 eV between the quartz and rutile modifications of GeO_2 [64]. However theoretical calculations showed that this chemical shift is not due to different atomic charges on four-fold and six-fold coordinated Ge atoms [64].

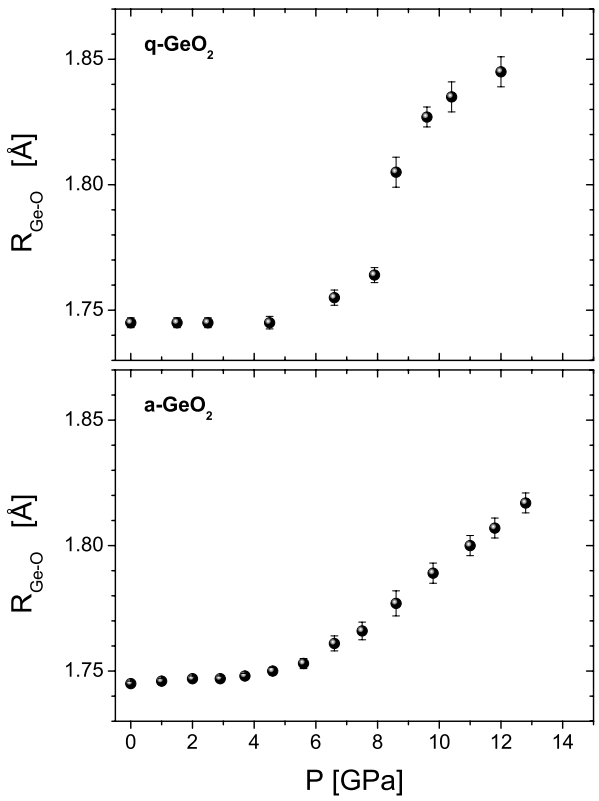

Figure 6. Evolution of the first shell Ge–O distance of crystalline (top panel) and amorphous (bottom panel) GeO_2 as a function of increasing pressure. See the text for discussion.

At low pressures, the Ge–O distance is practically constant with increasing pressure (figure 6, top panel). This is in contradiction with previous XAS [31] and MD [43] findings, which indicate a Ge–O bond contraction of about 0.01 Å in the pre-transition region. However, the present result is in agreement with older EXAFS measurements [65] limited to 5.8 GPa and finds a full explanation in previous neutron [66] and x-ray diffraction [67] data: the predominant bulk compression mechanism in q-GeO_2 is a distortion of the tetrahedra arising from changes in O–$\hat{\text{Ge}}$–O angles, so that the average Ge–O bond lengths are almost constant in spite of an overall decrease of lattice parameters as a function of pressure.

As is evident from both XANES spectra and EXAFS signals (figures 1 and 3, top panels), the phase transition is quite sharp and located at about 8.5 GPa. This is roughly in agreement with the findings of the previous XAS study [31] and MD calculations [43]. However, from both the edge position shift and Ge–O distance evolution (figures 2 and 6, top panels) it emerges that the transformation is not step-like and the whole 6–12 GPa range should be considered as the transition region. The four-fold to six-fold change is characterized by an increase of about 0.1 Å in the average Ge–O bond length. An interatomic distance of about 1.85 Å is reasonable for an octahedral configuration above 12 GPa, since at ambient pressure the six-fold coordinated rutile GeO_2 presents Ge–O bonds of about 1.88 Å [52].

The pressure behavior of germanium coordination number N (figure 7, top panel) qualitatively reflects the Ge–O distance

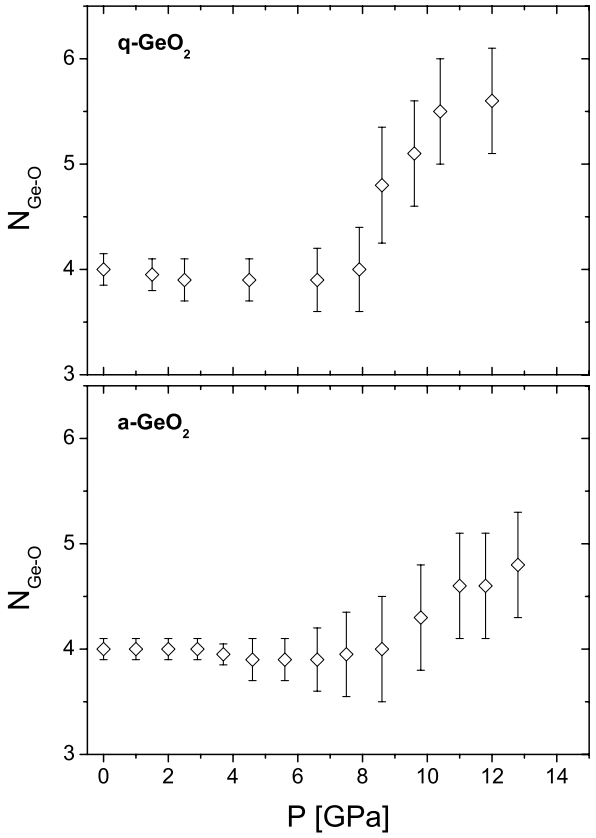

Figure 7. Evolution of the first shell Ge–O coordination number of crystalline (top panel) and amorphous (bottom panel) GeO_2 as a function of increasing pressure.

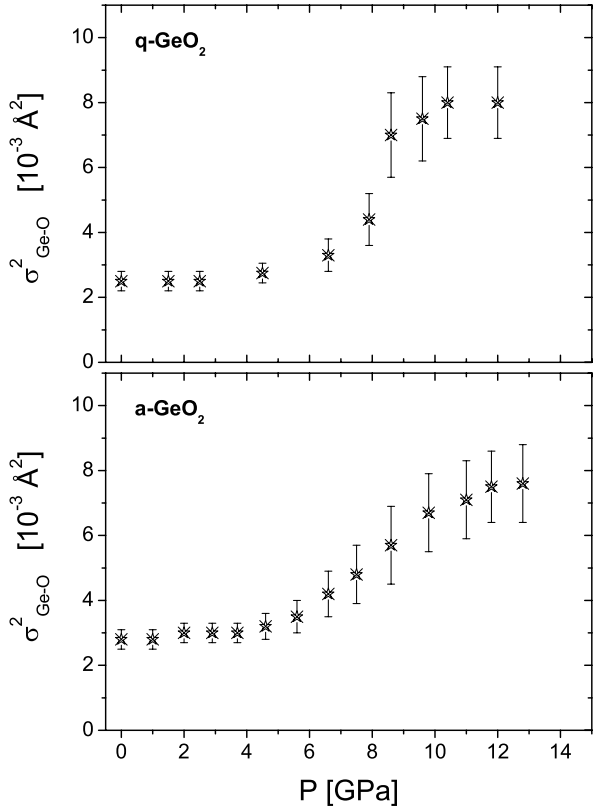

Figure 8. Evolution of the first shell Ge–O σ^2 of crystalline (top panel) and amorphous (bottom panel) GeO_2 as a function of increasing pressure.

evolution: it is constantly equal to $N = 4$ in the low pressure region, then it sharply increases and reaches a high pressure value compatible with $N \approx 6$. The increase in the number of oxygen nearest neighbors is accompanied by an increase in the bond length disorder, monitored by the σ^2 parameter, which undergoes a rough increase of about 0.005 Å^2 after the transition (figure 8, top panel). This agrees with the σ^2 pressure dependence obtained in [52] for q-GeO_2 up to 14 GPa. The σ^2 value at ambient conditions is about 0.0025 Å^2, in substantial agreement with results from a temperature dependent EXAFS study [68].

4.2. Amorphous GeO_2

4.2.1. Short range order. A qualitative inspection of XANES spectra and EXAFS signals (figures 1 and 3, bottom panels) already suggests that the structural modifications in a-GeO_2 are more sluggish with respect to quartz-like GeO_2. Indeed, the quantitative pressure behavior of both the edge position and the Ge–O interatomic distance (figures 2 and 6, bottom panels), confirms that the tetrahedral-to-octahedral transition in amorphous GeO_2 is much more gradual than in the crystalline compound and extends over a larger pressure range. The interatomic distance R_{Ge-O} is very slightly increasing up to about 5 GPa, then a more marked but gradual increase takes place up to about 1.82 Å at the maximum pressure reached. Once again, the Ge–O coordination number (figure 7, bottom panel) qualitatively follows the same pressure trend as R_{Ge-O}: it is roughly constant to $N = 4$ in the low pressure range, then gradually increases to reach only about $N \approx 5$ at 13 GPa. Also for a-GeO_2 the increase in local coordination is accompanied by a higher degree of structural disorder of bond lengths, monitored by the σ^2 parameter (figure 8, bottom panel). These findings are at variance with the previous XAS results [31, 32] and the following two-domain modeling [34], which propose quite a sharp transition, similar to q-GeO_2 and completed at about 13 GPa. The discrepancy is probably to be attributed to the higher quality and longer k-range of present experimental data.

Quite recently, an abrupt four- to six-fold coordination change was found in liquid germanate [69] at much lower pressures (around 3 GPa). This behavior was attributed to the absence of kinetic limitations for the liquid system. Kinetic effects of the AAT in a-GeO_2, consequent from the intrinsic metastability and non-ergodicity of amorphous systems, were investigated in [70].

A slower transition for a-GeO_2, reaching an octahedral coordination only at pressures well above 13 GPa, was predicted by MD simulations [41–43]. However, while Micoulaut *et al* [42] find a constant R_{Ge-O} up to about 9 GPa, Shanavas *et al* [43] obtain a rapid increase of R_{Ge-O} in the first few GPa followed by a constant bond length region. Clearly both these pressure behaviors of Ge–O distance proposed by MD are in disagreement with the present experimental findings (figure 6, bottom panel). Moreover, according to MD the fully

octahedral state is not observed even up to about 30 GPa and this seems reasonably incompatible with the evolution of Ge–O distance obtained in this work up to 13 GPa.

As a matter of fact, while experimental techniques like EXAFS or diffraction give access only to average quantities (distance, coordination number, etc), the possible coexistence of four-fold, five-fold and six-fold coordinated Ge atoms over a large pressure range was found by MD [43, 71] and cannot in principle be excluded. The formation of both five- and six-coordinated $^{[5]}$Ge and $^{[6]}$Ge atoms during the tetrahedral to octahedral high pressure transformation was firstly suggested by Raman scattering measurements [35]. However, the results of this work do not give evidence of any intermediate state with a constant average coordination of five between 6 and 10 GPa, as claimed from x-ray and neutron diffraction data [38]. Neither the double-step increase in coordination number at about 5 and 10 GPa [38] nor the fully octahedral state at 13 GPa [39, 40] can be confirmed by the Ge–O distance and coordination number (figures 6 and 7, bottom panels) pressure evolution found in the present study. Although it would be interesting to perform both EXAFS and diffraction measurements on exactly the same sample at the same pressure conditions, the very limited good Q-range of the *in situ* high pressure diffraction data (see figure 1 of [38]) should be taken into account in order to explain the discrepancies with present results.

4.2.2. Intermediate range order. As already mentioned above, below about 5 GPa the Ge–O distance is only very slightly changing and the coordination number is not increasing. Therefore in this pressure range the glass possibly experiences only a distortion and rotation of GeO_4 tetrahedra, as well as a modification of the inter-tetrahedral Ge–Ô–Ge angle which affects the IRO. Changes in Ge coordination number begin to take place only later, in agreement with density and Raman measurements [33, 39] as well as with diffraction findings on the densified GeO_2 glass [72, 73].

Upon compression to about 10 GPa the IRO, monitored by the EXAFS signal beyond the first Ge–O shell, is progressively lost (figure 4, bottom panel). This is in agreement with the conclusions drawn from the linear Q-shift of the FSDP measured by diffraction [39], i.e. a continuous breakdown of the IRO. Interestingly enough, after 10 GPa some apparent IRO reconstruction is evident from both EXAFS signals and their Fourier transform moduli (figures 3 and 4, bottom panels). This new IRO signal might be associated with Ge–Ge correlations which arise as edge- and face-sharing octahedra begin to form.

However, a fully quantitative interpretation of the EXAFS signal coming from IRO in the amorphous system cannot be performed in the framework of standard analysis methods. Indeed, for pressures greater than about 6 GPa, the system is made up of a mixture of tetrahedra, pentahedra and octahedra, whose relative weight and connectivity is not well established: in other words, beyond the first Ge–O shell the structural model of the glass is mostly unknown at high pressures. Furthermore, for distances greater than about 2.5 Å the Ge–O and Ge–Ge radial distribution functions are in principle no longer composed of well isolated peaks at all pressure values, but we may be in the presence of a continuous distribution of distances. Therefore a computer simulation is the only way to generate a cluster of atoms representing the amorphous system and suitable for the calculation of two- and three-body contributions that make up EXAFS signal. According to the above discussion, while the only reasonable analysis approach to IRO would probably be a simultaneous refinement of EXAFS and diffraction data-sets on the basis of a reverse Monte Carlo procedure, this is nowadays a challenge at high pressure and falls beyond the scope of the present work.

5. Conclusions

Local structural changes in amorphous and crystalline GeO_2 have been investigated as a function of pressure up to 13 GPa. We have obtained new high quality and accurate EXAFS results, which allow us to confirm or rule out in a quantitative and detailed way several models proposed in the last two decades. The main conclusions of this work are at variance with most of the previous experimental and/or theoretical findings and can be summarized as follows:

(i) in the low pressure range (below about 5 GPa) the behavior of both q- and a-GeO_2 is similar, with possible deformation and rotation of GeO_4 tetrahedra and the Ge–O bond not undergoing an average compression;
(ii) quartz-like GeO_2 undergoes a tetrahedral to octahedral transformation whose character is not step-like: while being located at about 8.5 GPa, at least the full 6–12 GPa pressure range should be considered as the transition region;
(iii) in amorphous GeO_2 the analogous low-density high-density structural change is not as sharp as previously found: it is actually quite continuous and gradual and the full octahedral state is not reached at 13 GPa as commonly believed;
(iv) while the contemporary presence of four-, five- and six-fold coordinated Ge atoms cannot be excluded over the whole pressure range, no evidence is provided for the recently claimed intermediate state with a constant average coordination of five in the 6–10 GPa pressure range;
(v) a continuous breakdown of intermediate range order in glassy GeO_2 is observed up to about 10 GPa.

These results shed new light into a highly debated subject and contribute to a deeper understanding of the detailed mechanisms underlying the AAT in glassy GeO_2. This work also stimulates further high pressure EXAFS investigations on systems showing interesting poly-amorphic transitions.

Acknowledgments

The European Synchrotron Radiation Facility (ESRF) is acknowledged for provision of in-house research beam time. The authors are grateful to Sebastien Pasternak, Adrien Rodrigues, Florian Perrin and Wilson Crichton for technical help, to Carmelo Prestipino for advice and to Sonia Pin for sample characterization through x-ray diffraction.

References

[1] Brazhkin V V and Lyapin A G 2003 *J. Phys.: Condens. Matter* **15** 6059
[2] McMillan P F 2004 *J. Mater. Chem.* **14** 1506
[3] Wilding M C, Wilson M and McMillan P F 2006 *Chem. Soc. Rev.* **35** 964
[4] McMillan P F, Wilson M, Wilding M C, Daisenberger D, Mezouar M and Greaves G N 2007 *J. Phys.: Condens. Matter* **19** 415101
[5] McMillan P F, Wilson M, Daisenberger D and Machon D 2005 *Nat. Mater.* **4** 680
[6] Daisenberger D, Wilson M, McMillan P F, Cabrera R Q, Wilding M C and Machon D 2007 *Phys. Rev.* B **75** 224118
[7] Di Cicco A, Congeduti A, Coppari F, Chervin J C, Baudelet F and Polian A 2008 *Phys. Rev.* B **78** 033309
[8] Wei Y X, Wang R J and Wang W H 2005 *Phys. Rev.* B **72** 012203
[9] Sato T and Funamori N 2008 *Phys. Rev. Lett.* **101** 255502
[10] McMillan P F 2006 *Nature* **441** 823
[11] Santoro M, Gorelli F A, Bini R, Ruocco G, Scandolo S and Crichton W A 2006 *Nature* **441** 857
[12] Angell C A 2004 *Annu. Rev. Phys. Chem.* **55** 559
[13] Leadbetter A J and Wright A C 1972 *J. Non-Cryst. Solids* **7** 37
[14] Desa J A E, Wright A C and Sinclair R N 1988 *J. Non-Cryst. Solids* **99** 276
[15] Cervinka L 1988 *J. Non-Cryst. Solids* **106** 291
[16] Price D L, Saboungi M–L and Barnes A C 1998 *Phys. Rev. Lett.* **81** 3207
[17] Hussin R, Dupree R and Holland D 1999 *J. Non-Cryst. Solids* **246** 159
[18] Salmon P S, Barnes A C, Martin R A and Cuello G J 2006 *Phys. Rev. Lett.* **96** 235502
[19] Salmon P S, Barnes A C, Martin R A and Cuello G J 2007 *J. Phys.: Condens. Matter* **19** 415110
[20] Giacomazzi L, Umari P and Pasquarello A 2005 *Phys. Rev. Lett.* **95** 075505
[21] Kohara S and Suzuya K 2005 *J. Phys.: Condens. Matter* **17** S77
[22] Hoang V V 2006 *J. Phys.: Condens. Matter* **18** 777
[23] Giacomazzi L, Umari P and Pasquarello A 2006 *Phys. Rev.* B **74** 155208
[24] Giacomazzi L and Pasquarello A 2007 *J. Phys.: Condens. Matter* **19** 415112
[25] Peralta J, Gutiérrez G and Rogan J 2008 *J. Phys.: Condens. Matter* **20** 145215
[26] Micoulaut M, Cormier L and Henderson G S 2006 *J. Phys.: Condens. Matter* **18** R753
[27] Majérus O, Cormier L, Itié J P, Galoisy L, Neuville D R and Calas G 2004 *J. Non-Cryst. Solids* **345/346** 34
[28] Coussa C, Martinet C, Champagnon B, Grosvalet L, Vouagner D and Sigaev V 2007 *J. Phys.: Condens. Matter* **19** 266220
[29] Cormier L, Ferlat G, Itié J P, Galoisy L, Calas G and Aquilanti G 2007 *Phys. Rev.* B **76** 134204
[30] Grimsditch M, Bhadra R and Meng Y 1988 *Phys. Rev.* B **38** 7836
[31] Itié J P, Polian A, Calas G, Petiau J, Fontaine A and Tolentino H 1989 *Phys. Rev. Lett.* **63** 398
[32] Vannereau F, Itié J P, Polian A, Calas G, Petiau J, Fontaine A and Tolentino H 1991 *High Pressure Res.* **7** 372
[33] Durben D J and Wolf G H 1991 *Phys. Rev.* B **43** 2355
[34] Smith K H, Shero E, Chizmeshya A and Wolf G H 1995 *J. Chem. Phys.* **102** 6851
[35] Polsky C H, Smith K H and Wolf G H 1999 *J. Non-Cryst. Solids* **248** 159
[36] Ishihara T, Shirakawa Y, Iida T, Kitamura N, Matsukawa M, Ohtori N and Umesaki N 1999 *Japan. J. Appl. Phys.* **38** 3062
[37] Teredesai P V, Anderson D T, Hauser N, Lantzky K and Yarger J L 2005 *Phys. Chem. Glasses* **46** 345
[38] Guthrie M, Tulk C A, Benmore C J, Xu J, Yarger J L, Klug D D, Tse J S, Mao H K and Hemley R J 2004 *Phys. Rev. Lett.* **93** 115502
[39] Hong X, Shen G, Prakapenka V B, Newville M, Rivers M L and Sutton S R 2007 *Phys. Rev.* B **75** 104201
[40] Hong X, Shen G, Prakapenka V B, Rivers M L and Sutton S R 2007 *Rev. Sci. Instrum.* **78** 103905
[41] Micoulaut M 2004 *J. Phys.: Condens. Matter* **16** L131
[42] Micoulaut M, Guissani Y and Guillot B 2006 *Phys. Rev.* E **73** 031504
[43] Shanavas K V, Garg N and Sharma S M 2006 *Phys. Rev.* B **73** 094120
[44] Sugai S and Onodera A 1996 *Phys. Rev. Lett.* 77 4210
[45] Hemley R J, Meade C and Mao H K 1997 *Phys. Rev. Lett.* **79** 1420
[46] Swenson J 1997 *Phys. Rev. Lett.* **79** 1421
[47] Sugai S and Onodera A 1997 *Phys. Rev. Lett.* **79** 1422
[48] Smith G S and Isaacs P B 1964 *Acta Crystallogr.* **17** 842
[49] Haines J, Cambon O, Philippot E, Chapon L and Hull S 2002 *J. Solid State Chem.* **166** 434
[50] Haines J, Léger J M and Chateau C 2000 *Phys. Rev.* B **61** 8701
[51] Prakapenka V P, Shen G, Dubrovinsky L S, Rivers M L and Sutton S R 2004 *J. Phys. Chem. Solids* **65** 1537
[52] Ohtaka O, Yoshiasa A, Fukui H, Murai K, Okube M, Katayama Y, Utsumi W and Nishihata Y 2001 *J. Synchrotron Radiat.* **8** 791
[53] Filipponi A, Borowski M, Bowron D T, Ansell S, Di Cicco A, De Panfilis S and Itié J P 2000 *Rev. Sci. Instrum.* **71** 2422
[54] Morard G, Mezouar M, Rey N, Poloni R, Merlen A, Le Floch S, Toulemonde P, Pascarelli S, San-Miguel A, Sanloup C and Fiquet G 2007 *High Pressure Res.* **27** 223
[55] Mezouar M, Le Bihan T, Libotte H, Le Godec Y and Häusermann D 1999 *J. Synchrotron Radiat.* **6** 1115
[56] Hammersley A P, Svensson S O, Thompson A, Graafsma H, Kvick Å and Moy J P 1995 *Rev. Sci. Instrum.* **66** 2729
[57] Crichton W A and Mezouar M 2002 *High Temp.—High Pressures* **34** 235
[58] Vinet P, Smith J R, Ferrante J and Rose J H 1987 *Phys. Rev.* B **35** 1945
[59] Le Godec Y, Martinez-Garcia D, Mezouar M, Syfosse G, Itié J P and Besson J M 2000 *High Pressure Res.* **17** 35
[60] Mezouar M, Faure P, Crichton W, Rambert N, Sitaud B, Bauchau S and Blattmann G 2002 *Rev. Sci. Instrum.* **73** 3570
[61] Ravel B and Newville M 2005 *J. Synchrotron Radiat.* **12** 537
[62] Klementev K V 2001 *J. Phys. D: Appl. Phys.* **34** 209
[63] Newville M 2001 *J. Synchrotron Radiat.* **8** 322
[64] Bertini L, Ghigna P, Scavini M and Cargnoni F 2003 *Phys. Chem. Chem. Phys.* **5** 1451
[65] Houser B, Alberding N, Ingalls R and Crozier E D 1988 *Phys. Rev.* B **37** 6513
[66] Jorgensen J D 1978 *J. Appl. Phys.* **49** 5473
[67] Yamanaka T and Ogata K 1991 *J. Appl. Cryst.* **24** 111
[68] Yoshiasa A, Tamura T, Kamishima O, Murai K, Ogata K and Mori H 1991 *J. Synchrotron Radiat.* **6** 1051
[69] Ohtaka O, Arima H, Fukui H, Utsumi W, Katayama Y and Yoshiasa A 2004 *Phys. Rev. Lett.* **92** 155506
[70] Tsiok O B, Brazhkin V V, Lyapin A G and Khvostantsev L G 1998 *Phys. Rev. Lett.* **80** 999
[71] Micoulaut M, Yuan X and Hobbs L W 2007 *J. Non-Cryst. Solids* **353** 1961
[72] Stone C E, Hannon A C, Ishihara T, Kitamura N, Shirakawa Y, Sinclair R N, Umesaki N and Wright A C 2001 *J. Non-Cryst. Solids* **293–295** 769
[73] Sampath S, Benmore C J, Lantzky K M, Neuefeind J, Leinenweber K, Price D L and Yarger J L 2003 *Phys. Rev. Lett.* **90** 135502